Electronic Supplementary Material (ESI) for Journal of Materials Chemistry B.

Supporting Information

Fluorescence Diagnose of Pneumonia with an ultra-sensitive Two-Photon Near-Infrared Fluorescent Probe

Erwang Song,[a] Youbo Lai,[a] Huixu Lu,[a] Yonghe Tang,[a] Lintao Zeng, *[b] and Weiying Lin, *[, a]

[a] Guangxi Key Laboratory of Electrochemical Energy Materials, Institute of Optical Materials and Chemical Biology, School of Chemistry and Chemical Engineering, Guangxi University, Nanning, 530004, China. E-mail: weiyinglin2013@163.com.

[b] School of Light Industry and Food Engineering, Guangxi University, Nanning, 530004, China. E-mail: zlt1981@126.com.

Table of contents

1. Materials

Isophorone, malononitrile, 4-methylpiperidine, 3-quinolinecarboxaldehyde, methyl trifluoromethane sulfonate, C_2H_5OH, CH_2Cl_2 and DMSO were of analytical grade, which were purchased from HeownsReagent and used directly without further purification.

2. Reagents and instruments

Unless otherwise stated, all chemicals were purchased from commercial suppliers and were used without further purification. Solvents were purified before use.

Human breast cancer cells MCF-7 and human cervical cancer HeLa were purchased from the Tongpai (Shanghai) Biotechnology Co., Ltd. Dulbecco's modified Eagle's medium (DMEM, C11875500CP) and fetal bovine serum (FBS) were obtained from Gibco Invitrogen Corp._^{1}H NMR and ^{13}C NMR spectra were recorded on a Bruker AVANCEIII spectrometer at room temperature (Bruker, Billerica, MA). High-resolution mass spectra (HRMS) were recorded on a HP-1100 LC-MS Spectrometer. UV-vis absorption spectra was measured with a SHIMADZU UV-800 spectrophotometer. Hitachi F-900 fluorescence spectra was determined to measure fluorescence spectra. The fluorescence images of MCF-7 cells and HeLa cells and tissue slice of mice were recorded on a Nikon A1 confocal laser scanning microscope (CLSM).

3. Synthesis of probe

3.1 Synthesis of DCI

Isophorone (1.6 mL, 10.6 mmol) and malononitrile (841.6 mg, 12.7 mmol) were added into a 100 mL three-necked round bottom flask, and then was completely dissolved by adding 10

mL of absolute ethanol. Finally, 2 drops of 4- Methyl piperidine were added as a catalyst. The mouth of the flask was equipped with a spherical condenser and the mixture was heated and refluxed for 24 hours in a nitrogen atmosphere at 78 ℃. After the reaction completed, we stopped heating. The crude product was purified by silica gel column chromatography with ethyl acetate and petroleum ether (v/v = 1/6) as the eluent. The solvent was removed under reduced pressure on a rotary evaporator and then we obtained white crystals dicyanoisophorone (1.4950 g, yield 82%).

^{1}H NMR (500 MHz, CD_3OD-d_4) δ/ppm 7.38 (s, 1H, CH), 3.33 (s, 2H, CH_2), 3.04 (s, 2H, CH_2), 2.83 (s, 3H, CH_3), 1.80 (s, 6H, CH_3).

^{13}C NMR (126 MHz, CD_3OD-d_4) δ/ppm 172.3, 162.5, 121.1, 114.2, 113.5, 78.5, 46.3, 43.5, 33.2, 27.9, 25.3

3.2 Synthesis of DCIQ

Dicyanoisophorone (150.0 mg, 0.9 mmol) and 3-quinolinecarboxaldehyde (137.1 mg, 0.9 mmol) were added into a 100 mL three-necked round bottom flask, then they were completely dissolved by adding 10 mL of absolute ethanol. Finally, 2 drops of 4-methylpiperidine were added as a catalyst. The mouth of the flask was equipped with a spherical condenser and the mixture was heated and refluxed for 4 hours in a nitrogen atmosphere at 78 ℃. After the reaction was completed, we stopped heating. After the reaction solution was cooled to room temperature, a yellow solid gradually precipitated. The liquid was removed by vacuum filtration and the filter cake was washed with cold ethanol. After drying, we obtained a yellow fluffy needle-like solid DCIQ (240.9 mg, yield 84.6%).

^{1}H NMR (500 MHz, $CDCl_3$) δ/ppm 9.10 (d, *J* = 1.8 Hz, 1H, Ar-H), 8.34 (s, 1H, Ar-H), 8.20 (d, *J* = 8.0 Hz, 1H, Ar-H), 7.90 (d, *J* = 7.0 Hz, 1H, Ar-H), 7.80 (t, *J* = 7.5 Hz, 1H, Ar-H), 7.65 (t, *J* = 7.5 Hz, 1H, Ar-H), 7.24 (d, *J* = 6.5 Hz, 2H, =CH), 6.98 (s, 1H, =CH), 2.67 (s, 2H, CH_2), 2.56 (s, 2H, CH_2), 1.14 (s, 6H, CH_3).

^{13}C NMR (126 MHz, $CDCl_3$) δ/ppm 169.0, 152.8, 149.4, 148.0, 134.0, 133.1, 131.1, 130.6, 129.3, 128.8, 128.3, 127.9, 127.6, 124.6, 113.3, 112.5, 79.9, 43.0, 39.2, 32.1, 29.7, 28.1.

3.3 Synthesis of DCQN:

DCIQ (56.4 mg, 0.173 mmol) and methyl trifluoromethanesulfonate (80 μL, 0.708 mmol) were added into a dry 100 mL single-necked round bottom flask, and then was completely

dissolved by adding 10 mL of dry dichloromethane. The reaction was stirred for 12 h in a nitrogen atmosphere at room temperature, and a yellow solid gradually precipitated. After the reaction was completed, the liquid was removed by vacuum filtration and the filter cake was washed with cold dichloromethane. After drying, we obtained a yellow solid product DCQN (80.7 mg, yield 95.0 %).

^{1}H NMR (500 MHz, DMSO-d_6) δ/ppm 9.89 (s, 1H, Ar-H), 9.41 (s, 1H, Ar-H) 8.51 (d, *J* = 8.9 Hz, 1H, Ar-H), 8.40 (d, *J* = 7.6 Hz, 1H), 8.27 (d, *J* = 8.7 Hz, 1H, Ar-H), 8.07 (t, *J* = 7.6 Hz, 1H, Ar-H), 7.78 (d, *J* = 16.3 Hz, 1H, =CH), 7.53 (d, *J* = 16.3 Hz, 1H, =CH), 6.97(s, 1H, =CH), 4.64(s, 6H, CH_3), 2.71(s, 2H, CH_2), 2.61(s, 2H, CH_2), 1.07(s, 6H, CH_3).

^{13}C NMR (126 MHz, DMSO-d_6) δ/ppm 170.4, 154.1, 150.1, 143.8, 137.9, 136.0, 134.9, 131.1, 131.0, 130.7, 129.5, 125.6, 122.4, 119.8, 113.8, 113.2, 79.5, 46.2, 42.6, 38.5, 32.2, 27.8.

4. Mechanism of the DCQN sensing of HSO_3^-

In order to explore the mechanism of reaction of DCQN with HSO_3^-, we conducted ^{1}H NMR titration experiments and HRMS analysis. As shown in Fig. S1, the signals at chemical shifts of 9.62 ppm and 9.27 ppm in Fig. S1-b correspond to H_a and H_b in Fig. S1-a. When the probe was reacted with 18 equivalents of HSO_3^-, the chemical shifts of H_a and H_b moved to upfield chemical shifts of 6.42 ppm and 4.93 ppm, respectively. In addition, the methyl proton signal (H_c) originating from position 1 of the quinolinium group also moved from 4.57 ppm to 3.32 ppm. These results indicate that the quinolinium group in DCQN may have undergone a 1,4-nucleophilic addition reaction with HSO_3^-, resulting in the destruction of the original A-π-A structure of DCQN and the formation of DCQN-SO_3H with a D-π-A structure. This D-π-A structure is compatible with the ICT effect, leading to NIR fluorescence activity. In the HRMS spectrum (Fig. S15), the main peak with an m/z value of 420.1389, confirmed the structure of DCQN-SO_3H. These results demonstrated the 1,4-Michael addition reaction between the quinolinium group and HSO_3^-, resulting in a hyperchromic reaction that leads to enhanced NIR fluorescence.

5. Preparation of solutions of probe DCQN and analytes

Unless otherwise noted, all the measurements were made according to the following

procedure. A stock solution of probe (1.0 mM) was prepared by dissolving the requisite amount of DCQN in DMSO. In a 10 mL tube, the test solution was prepared by placing 0.9 mL DMSO, 0.1 mL DCQN (1.0 mM), an appropriate volume of $NaHSO_3$ sample solution and adjusting the final volume to 10 mL with 0.1 M PBS (pH 7.4 or other different pH). 3 mL portion of it was transferred to a 1 cm quartz cell to measure absorbance or fluorescence. The stock solutions of analytes for selectivity experiments were prepared respectively by dissolving Na_2HPO_4, NaCl, $Zn(OAc)_2$, KH_2PO_4, KI, $NaHCO_3$, $MgSO_4$, HClO, NaClO, $NaNO_2$, $Ca(NO_3)_2$, GSH, L-Cys, Hcy, NaHS, Na_2S, $NH_3·H_2O$, putrescine, $EtNH_2$, 4-picoline, Et_2NH, $N_2H_4·H_2O$, Et_3N, N,N-diisopropylethylamine, H_2O_2, glucose, $NaHSO_3$ in ultrapure water.

6. Determination of the fluorescence quantum yield

In the determination of fluorescence quantum yield (Φ), Cy 5.5 which has Φ = 0.28 in PBS buffer (pH 7.4) was used as a fluorescence reference. The Cy 5.5 and the reaction product (DCQN-SO3H) were dissolved in PBS (pH 7.4), while an absorbance of ca. 0.05 of Cy5.5 was obtained by adjusting its concentration, we measured the fluorescence emission spectrum at the maximum excitation wavelength and the integrated areas of the spectra were calculated. Then, the fluorescence quantum yield was determined according to the following equation:

$$\Phi_{FS} = \Phi_{FR} (A_R F_S / A_S F_R) (\eta_S / \eta_R)^2$$

Where Φ is the fluorescence quantum yield, A is the absorbance at the maximum absorption wavelength, F is the integral area of the fluorescence spectrum, and η is the refractive index of the solvent. The subscripts S and R represent the analyteand the reference.

7. Determination of the detection limit

The calibration curve was first obtained from the plot of fluorescence F_{660} as a function of HSO_3^- level. The regression curve equation was obtained for the lower concentration part. And the result was shown in Fig. S4.

$$\text{Detection limit (LOD)} = 3 \times \sigma / k$$

where k is the slope of the curve equation, and σ represents the standard deviation for the fluorescence intensity of the probe in the absence of phosgene.

$$F_{660} = 424.3 + 23296.6 \times [HSO_3^-] \ (R^2 = 0.9998)$$

$$\text{Detection limit (LOD)} = 3 \times 11.60197347 / 23296.6 = 1.494 \text{ nM}$$

8. Cell culture

MCF-7 cells and HeLa were cultured in DMEM, supplemented with 10% FBS, 1%

streptomycin sulphate, 1% penicillin in a humidified 5% CO_2/ 95% air incubator at 37 ℃. Replace the growth medium every two days. When the cells had grown to 80%, they were digested with trypsin and then subcultured prior to experiments.

9. Cytotoxicity assay

The cytotoxicity of DCQN in MCF-7 cells was evaluated by using the CCK-8 (Shanghai Biyuntian Bio-Technology Co., Ltd.). MCF-7 cells were grown in 96-well plates (Corning) at 5000 cells per well. After the cells completely attached to the plates for 24 h, each well was washed with 100 μL PBS, and then incubated with various concentrations of DCQN (2.5, 5, 10, 15, 20, and 25 μM) for 24 h. Afterwards, each well was washed with 100 μL PBS and added 100 μL serum-free DMEM containing 10% CCK-8, and further incubated for 1 h, Finally, the absorbance at 450 nm was determined by a plate reader (Bio Tek: Gene Co., Ltd). As shown in Fig. S7, after incubating MCF-7 cells with various concentrations of **DCQN** (2.5, 5, 10, 15, 20 and 25 μM) for 24 h, the cell survival rate remained above 87%, these results suggested that **DCQN** has good biocompatibility.

10. Mitochondria-targeting ability of DCQN

Since the endogenous SO_2 is mainly produced in the mitochondria of cells, and the survival time in the cell is relatively short. In order to monitor endogenous SO_2 in cells effectively and accurately, the most ideal method is to develop mitochondrial-targeted in situ activated fluorescent light-up probes. In order to explore the mitochondrial targeted activation performance of **DCQN**, we incubated MCF-7 cells with 10 μM **DCQN** and the commercially available Mito-Tracker Green (200 nM) for 30 min at 37 ℃, and then the cells were incubated with HSO_3^- (60 μM) for 30 min. The excess probes were washed away with PBS, then the cells were scanned with a laser confocal microscope and their fluorescence images were recorded. As shown in Fi g. S8, clear and strong fluorescence profiles of mitochondria could be observed in the red channel, indicating that **DCQN** can respond to HSO_3^- in living cells and produce near-infrared fluorescence. By superimposing and comparing the fluorescence images under red channel and the Mito-Tracker Green channel, we found that the fluorescence images can overlap essentially perfectly with a high Pearson's correlation coefficient 0.95. These results

indicated that **DCQN** is a good mitochondrial targeted in-situ activated fluorescent probe, which can achieve high-contrast fluorescence imaging of intracellular SO_2.

11. Cell fluorescence imaging

Before exogenous SO_2 imaging, HeLa cells were added 10 μM DCQN and incubated for 30 min, and then imaged on a laser confocal microscope. Different concentrations of $NaHSO_3$ was added to the medium containing DCQN (10 μM) for 30 min. Under the excitation of 550 nm laser for one-photon imaging and 1100 nm laser for two-photon imaging, fluorescence images were acquired at the red channel (610− 710 nm). For the imaging of endogenous SO_2, the HeLa cells were divided into four groups. For first group, the cells were incubated with DCQN (10 μM) for 30 min. In the second group, the cells were cultured with LPS (0.1 mg/mL) for 30 min, then incubated with DCQN (10 μM) for 30 min before imaging. In the third group, the cells were pre-treated with LPS (0.1 mg/mL) for 30 min, and then treated with FA (2 mg/mL) for another 30 min, and then DCQN (10 μM) was added for 30 min incubation before imaging. In the fourth group, the cells were pre-treated with LPS (0.1 mg/mL) for 30 min, and then treated with crystapen (2 mg/mL) for another 30 min, and then DCQN (10 μM) was added for 30 min incubation before imaging.

12. Animal models and experiments in vivo

The four-weeks old female Kunming mice used for in vivo imaging were obtained from School of Pharmaceutical Sciences, Guangxi Medical University, and the studies were approved by the Animal Ethical Experimentation Committee of Guangxi Medical University. All animals were kindly kept during experiment according to the requirements of the National Act on the use of experimental animals (China).

For the imaging of exogenous SO_2, the mice were shaved belly hair with electric shaver and anesthetized by 4% chloral hydrate before imaging. Then **DCQN** (10 μM) was injected subcutaneously and imaged. After that, different concentrations of $NaHSO_3$ was injected and imaged.

For the imaging of endogenous SO_2, the mice were divided into three groups. In the first group, mice were pre-injected subcutaneously with LPS (100 μg/mL) for 24 h. Then **DCQN** (10 μM) was injected subcutaneously and imaged. In the second group, mice were pre-injected

subcutaneously with LPS (100 μg/mL) for 24 h and then pre-injected subcutaneously with FA (2 mg/mL) for 6 h. Then **DCQN** (10 μM) was injected subcutaneously and imaged. In the third group, mice were pre-injected subcutaneously with LPS (100 μg/mL) for 24 h and then pre-injected subcutaneously with penicillin sodium (2 mg/mL) for 6 h. Then **DCQN** (10 μM) was injected subcutaneously and imaged. λ_{ex} = 550 nm, λ_{em} = 660 nm.

13. Pneumonia mice lung slice preparation and imaging

The four-weeks old female Kunming mice were divided into four groups. The mice of group (a) were cultured normally as a reference. For other three groups (b, c and d), the mice were instilled with LPS (100 μg/mL) through the nasal cavity for three consecutive days. Then, the mice were sacrificed by cervical vertebra dislocation and the lung tissue was removed. Next, the lung tissue was cut into 1 mm sections. In groups (a and b), lung slices were treated with 10 μM **DCQN** for 3 h and imaged. In groups (c and d), lung slices were separately treated with FA (2 mg/mL) and penicillin sodium (2 mg/mL) for 3 h. Then lung slices were treated with 10 μM **DCQN** for another 3 h and imaged.

14. Hepatitis mice liver slice preparation and imaging

The four-weeks old female Kunming mice were divided into four groups. The mice of group (a) were cultured normally as a reference. For other three groups (b, c and d), the mice were injected with LPS (100 μg/mL) by intraperitoneal injection for three consecutive days. Then, the mice were sacrificed by cervical vertebra dislocation and the liver tissue was removed. Next, the lung tissue was cut into 1 mm sections. In groups (a and b), liver slices were treated with 10 μM **DCQN** for 30 min and imaged. In groups (c and d), liver slices were separately treated with FA (2 mg/mL) and penicillin sodium (2 mg/mL). Then liver slices were treated with 10 μM **DCQN** for 30 min and imaged. The result was shown in Fig. S9.

Table. S1. Comparison of fluorescent probes for SO_2 derivatives.

Fluorescent probes for SO_2	Excitation	Emission	Stokes shift	LOD	Response time	References
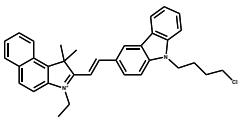	510→ 322 nm	588→462 nm	126 nm	10 nM	40 s	1
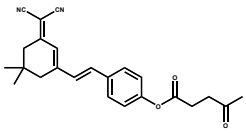	560 nm	695 nm	135 nm	70 μM	130 s	2
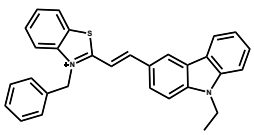	345 nm	483→600 nm	117 nm	161 nM	35 s	3
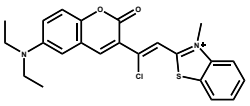	460 nm	490→749 nm	259 nm	1220 nM	5 min	4
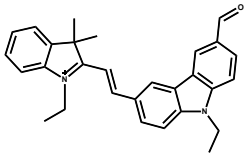	365 nm	445→570 nm	125 nm	1290 nM	1.5 min	5
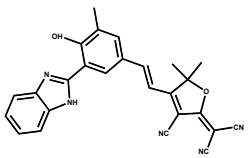	400 nm	482→664 nm	152 nm	82 nM	8 min	6
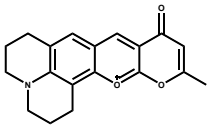	490 nm	537→590 nm	53 nm	440 nM	7 min	7
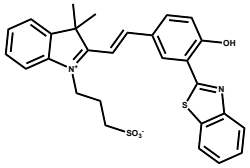	390 nm	450→590 nm	140 nm	340 nM	15 min	8
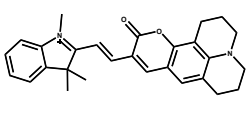	470 nm	515→680 nm	165 nm	530 nM	6 min	9

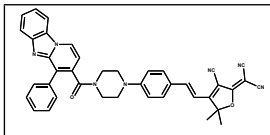	380 nm	465→640 nm	175 nm	62 nM	2 min	10
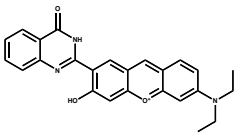	388 nm	566→450 nm	116 nm	44 nM	30 s	11
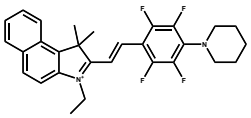	470 nm	465→592 nm	127 nm	3 nM	2 min	12
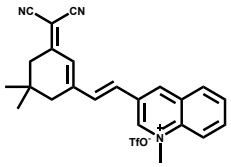	**550 nm**	**660 nm**	**110 nm**	**1.49 nM**	**6 s**	**This work**

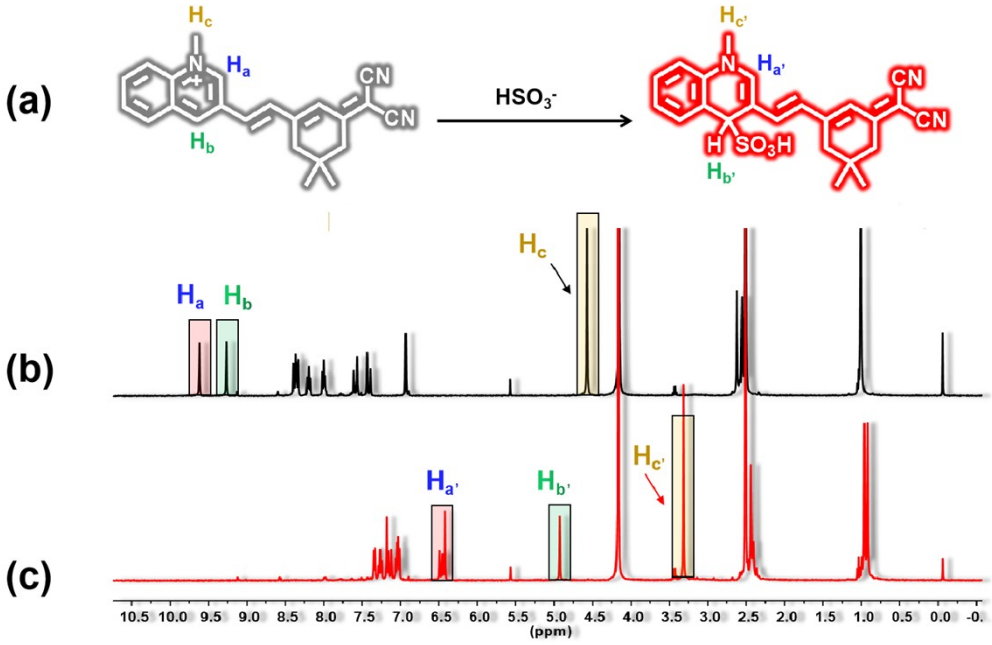

Fig. S1. (a) The sensing mechanism of DCQN towards HSO_3^-. ^1H NMR spectra of DCQN with (b) 0 equiv and (c) 18 equiv of HSO_3^- in DMSO-d_6.

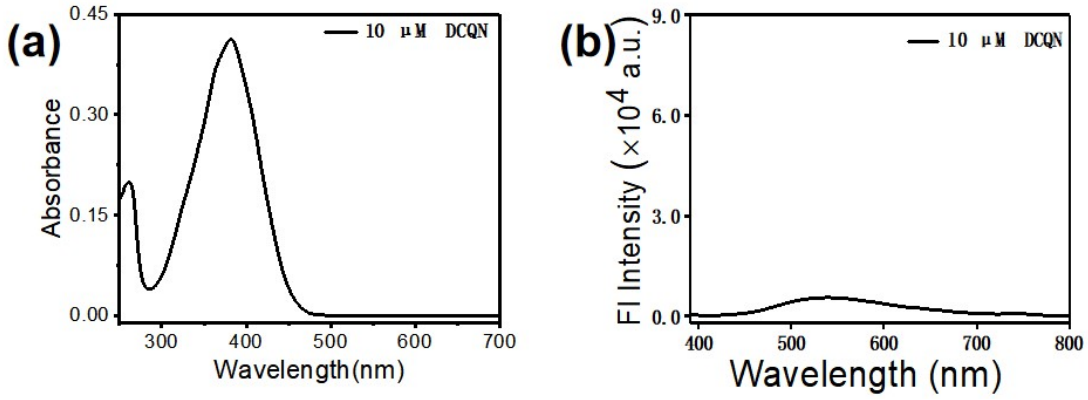

Fig. S2. (a) UV–vis absorption spectra and (b) fluorescence spectra of **DCQN** (10 μM) in aqueous solution (DMSO/PBS = 1/9, v/v, pH 7.4). λ_{ex} = 380 nm, slits: 2.5/2.5 nm. The error bars represent ± SD, n = 3.

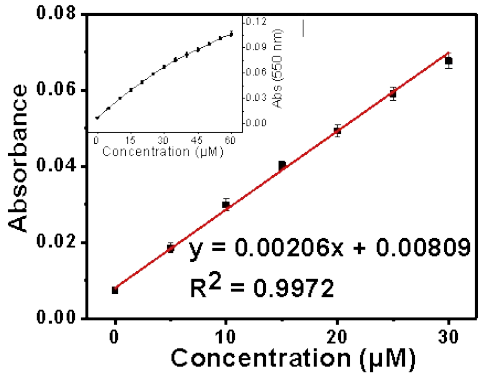

Fig. S3. Linear relationships between the absorbance of **DCQN** (10 μM) and the concentrations of sulfite. λ_{ex} = 550 nm, λ_{em} = 660 nm, slits: 2.5/2.5 nm. The error bars represent ± SD, n = 3.

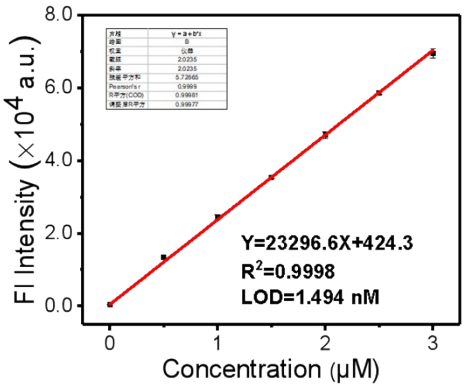

Fig. S4. The calibration curve of fluorescence intensity (F_{660}) of **DCQN** (1.0 μM) as a function of HSO_3^- concentration.

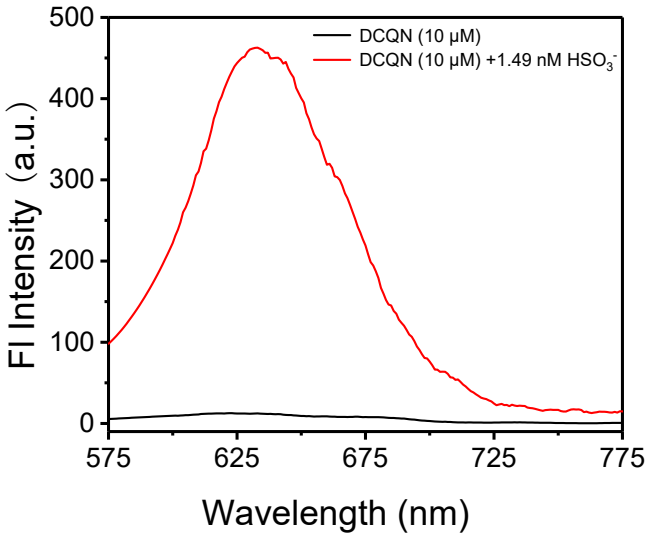

Fig. S5. Fluorescence spectra of **DCQN** (10 μM) after the addition of HSO_3^- (1.49 nM) in an aqueous solution (DMSO/PBS = 1/9, v/v, pH 7.4). λ_{ex} = 550 nm, slits: 2.5/2.5 nm.

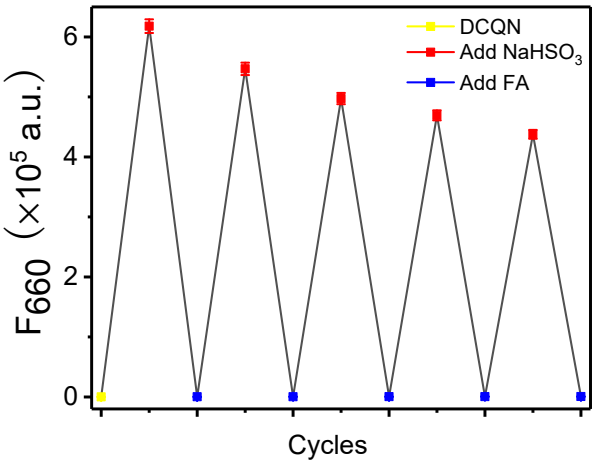

Fig. S6. Fluorescence response cycle experiments of DCQN (10 μM) with $NaHSO_3$ (60 μM) and formaldehyde solution (180 μM).

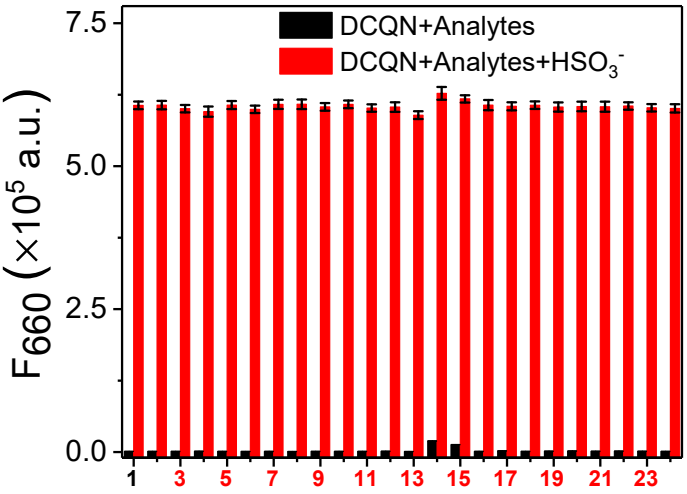

Fig. S7. Fluorescence response of **DCQN** for HSO_3^- in the co-presence of various analytes which include (1) Black, (2) Na_2HPO_4, (3) NaCl, (4) $Zn(OAc)_2$, (5) KH_2PO_4, (6) KI, (7) $NaHCO_3$, (8) $MgSO_4$, (9) $NaNO_2$, (10) $Ca(NO_3)_2$, (11) GSH, (12) L-Cys, (13) Hcy, (14) NaHS, (15) Na_2S, (16) $NH_3 \cdot H_2O$, (17) Putrescine, (18) $EtNH_2$, (19) 4-picoline, (20) Et_2NH, (21) $N_2H_4 \cdot H_2O$, (22) Et_3N, (23) N,N-diisopropylethylamine, (24) Glucose. λ_{ex} = 550 nm, λ_{em} = 660 nm, slits: 2.5/2.5 nm. The error bars represent ± SD, n = 3.

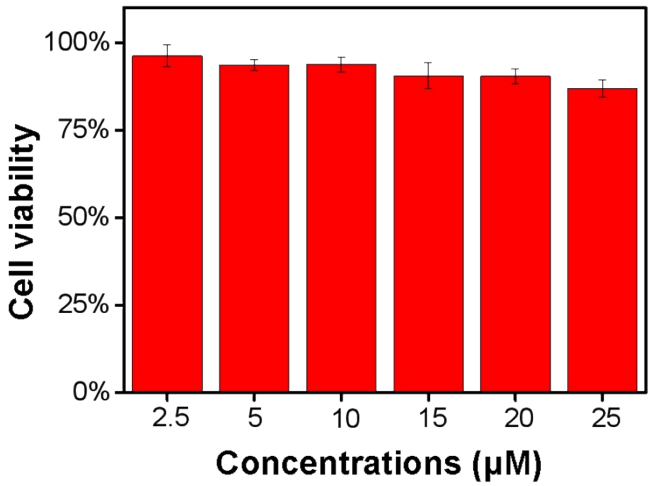

Fig. S8. Cell viability of MCF-7 after incubation with various concentrations of **DCQN** (0–25 μM) for 24 h. Error bars are ± SD, n = 5.

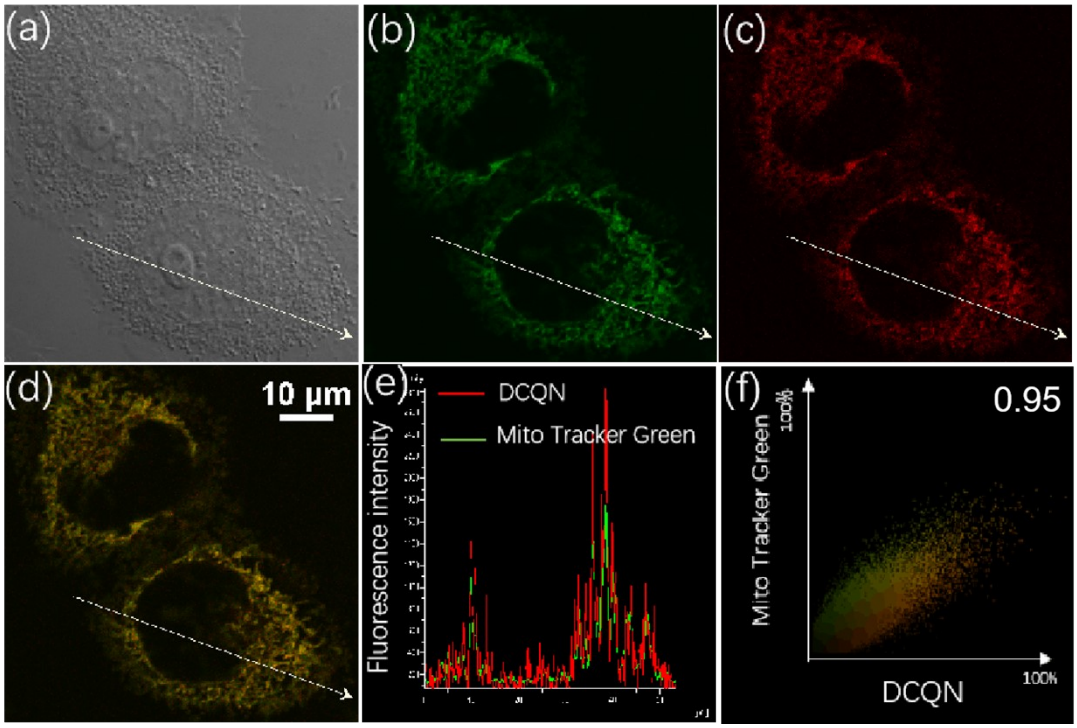

Fig. S9. Confocal images of MCF-7 cells stained with (b) 200 nM Mito-Tracker Green (green channel $\lambda_{ex}/\lambda_{em}$ of 488/500–530 nm) and (c) 10 μM **DCQN** (red channel $\lambda_{ex}/\lambda_{em}$ of 550/610–710 nm) for 30 min and then further incubated with HSO_3^- (60 μM) for another 10 min in MCF-7 cells. (a) Bright filed, (d) merged images, (e) intensity profile within the regions of interest, and (f) a correlation plot of Mito-Tracker Green and **DCQN** intensities. Pearson's correlation coefficient: 0.95. Scale bar: 10 mm.

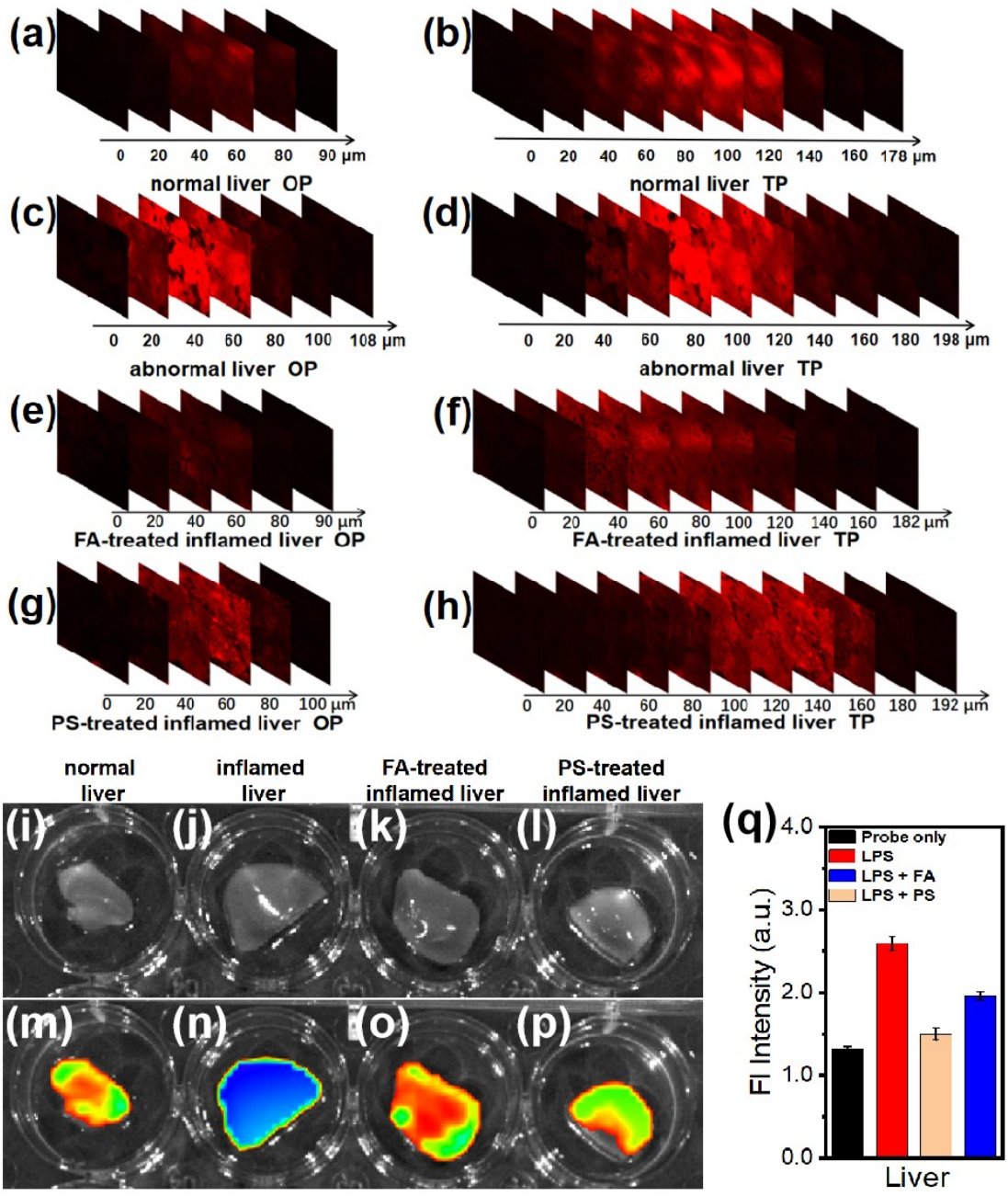

Fig. S10. (a) One-photon and two-photon Z-scan confocal fluorescence imaging of liver tissue of mice. The first row: fluorescence image of normal mouse liver tissue after incubation with DCQN (10 μM) for 3 h; The second row: fluorescence image of inflamed liver tissue after incubation with DCQN (10 μM) for 3 h; The third row: fluorescence image of inflamed liver tissue treated with FA (2 mg/mL) for 3 h, and then further incubated with DCQN (10 μM) for another 3 h; The forth row: fluorescence image of inflamed liver tissue treated with

Benzylpenicillin Sodium (2 mg/mL) for 3 h, and then further incubated with DCQN (10 μM) for another 3 h. For one-photon excitation: λex = 550, λem = 610–710 nm; For two-photon excitation: λex = 1100, λem = 610–710 nm. Scale bar: 20 μm.

(b) Photograph of liver tissue of mice in the experiment without excitation (the first row) and under the irradiation of λex = 550, λem = 660 nm (the second row). (c) Statistical analysis based on fluorescence intensity of liver tissue. Error bars represent ± SD, n = 3.

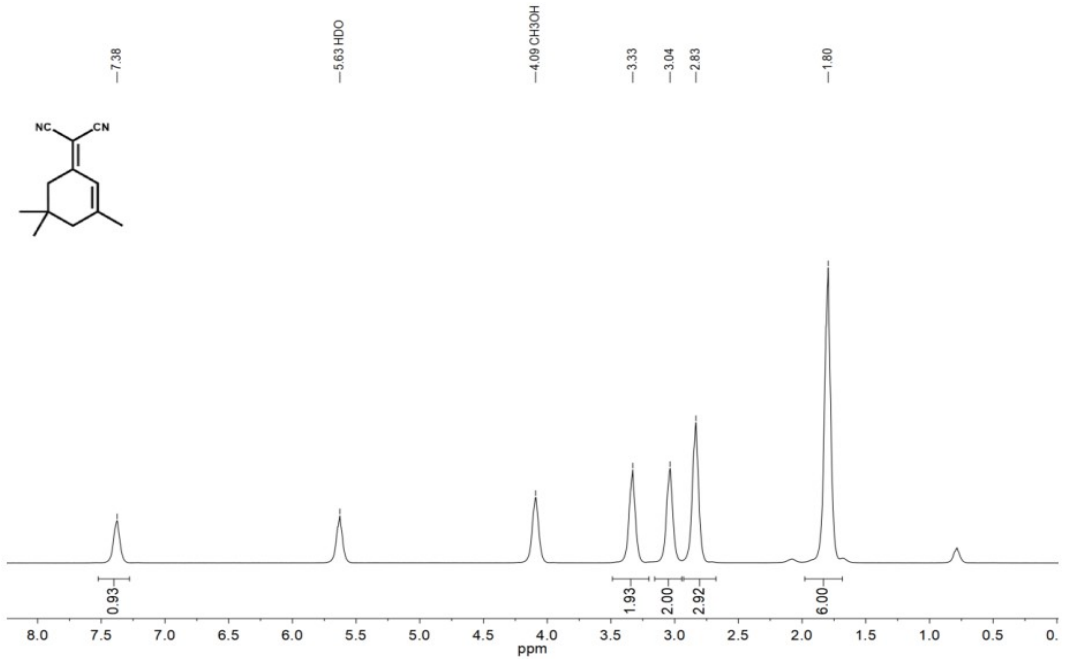

Fig. S11. ^{1}H NMR spectrum of compound 1 in CD_3OD-d_4 (500 MHz).

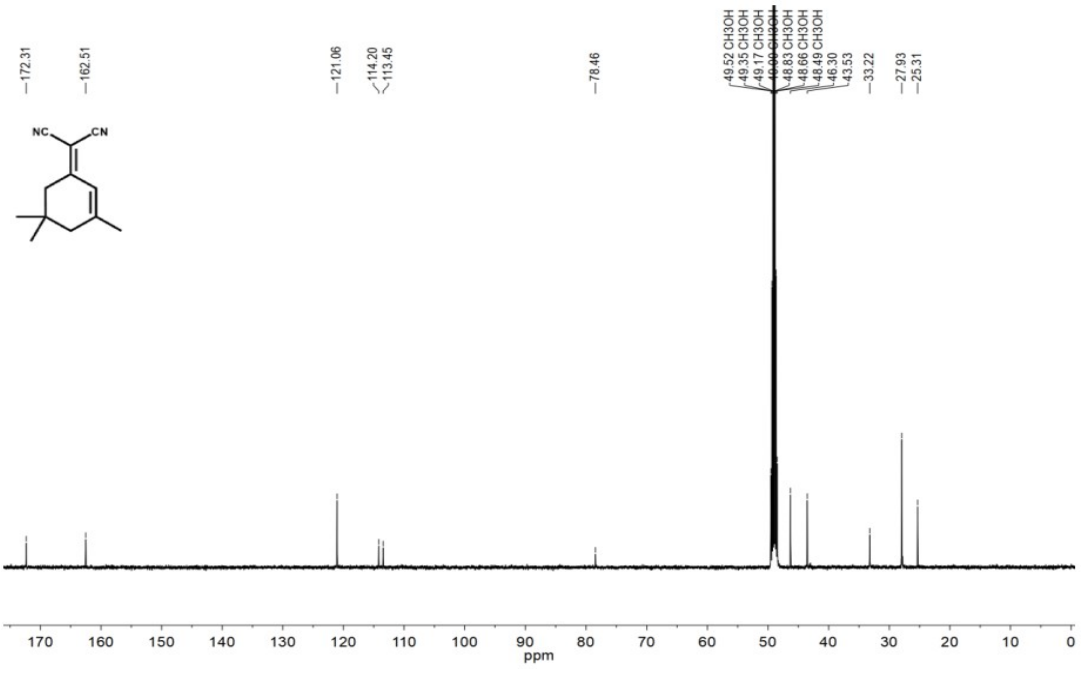

Fig. S12. ^{13}C NMR spectrum of compound 1 in CD_3OD-d_4 (126 MHz).

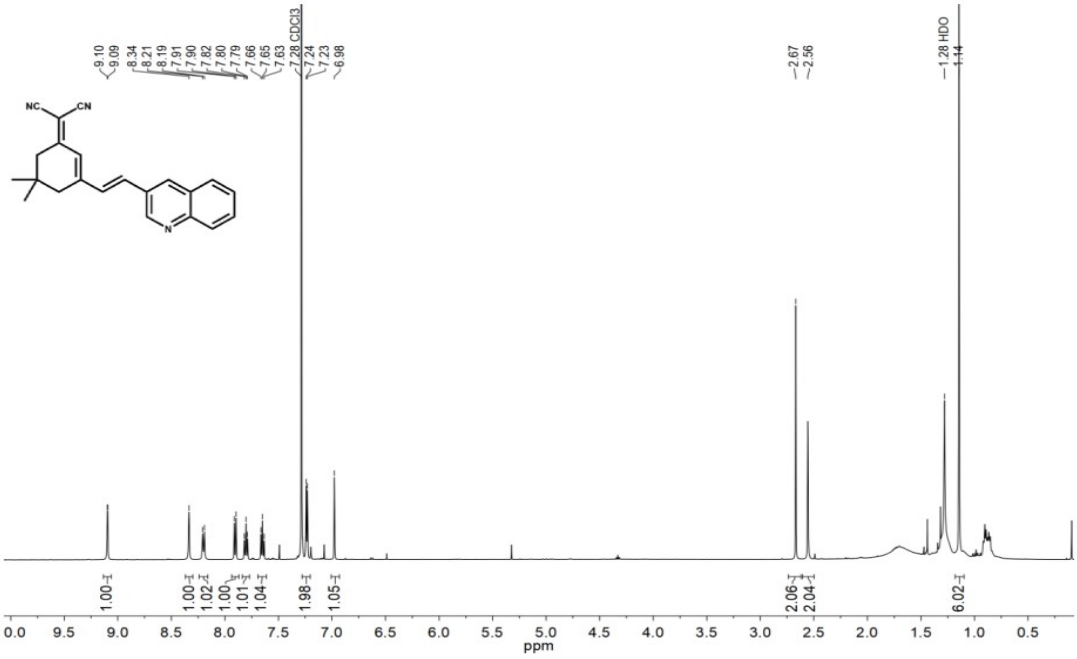

Fig. S13. ^{1}H NMR spectrum of compound 2 in $CDCl_3$ (500 MHz).

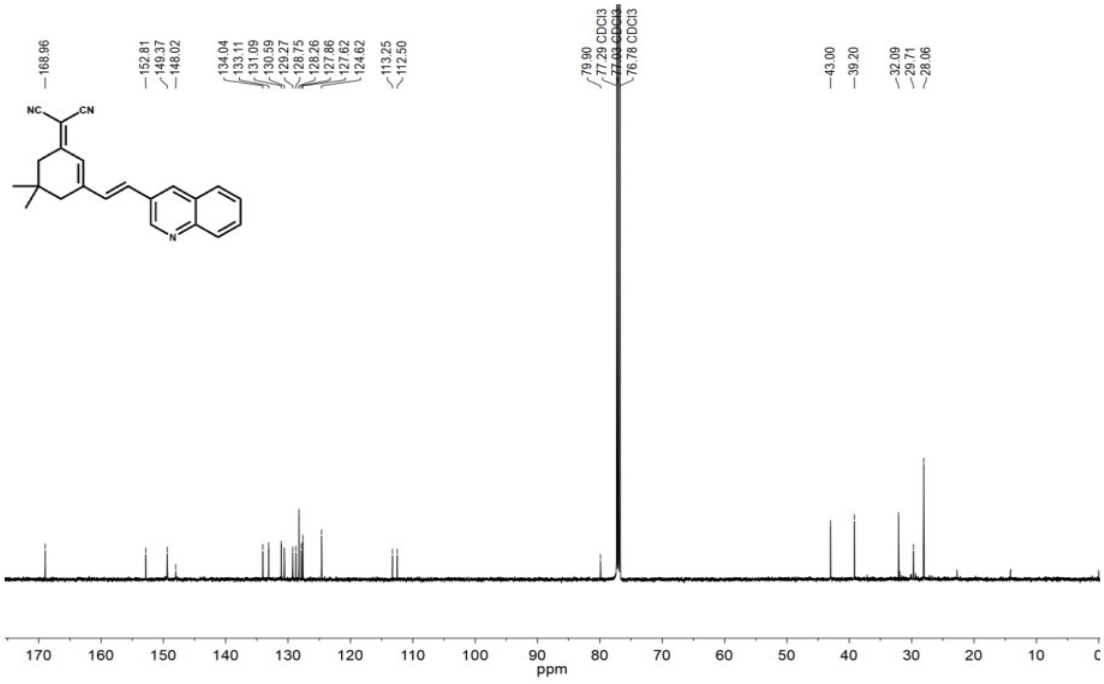

Fig. S14. ^{13}C NMR spectrum of compound 2 in $CDCl_3$ (126 MHz).

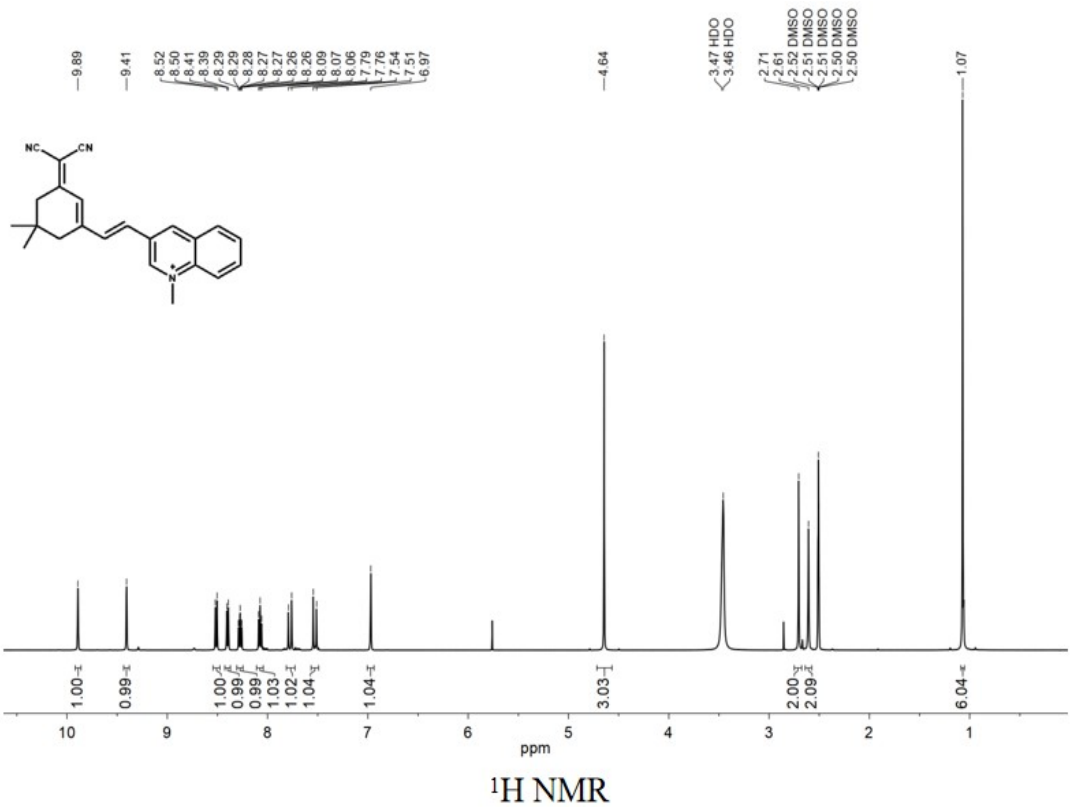

Fig. S15. ^{1}H NMR spectrum of **DCQN** in DMSO-d_6 (500 MHz).

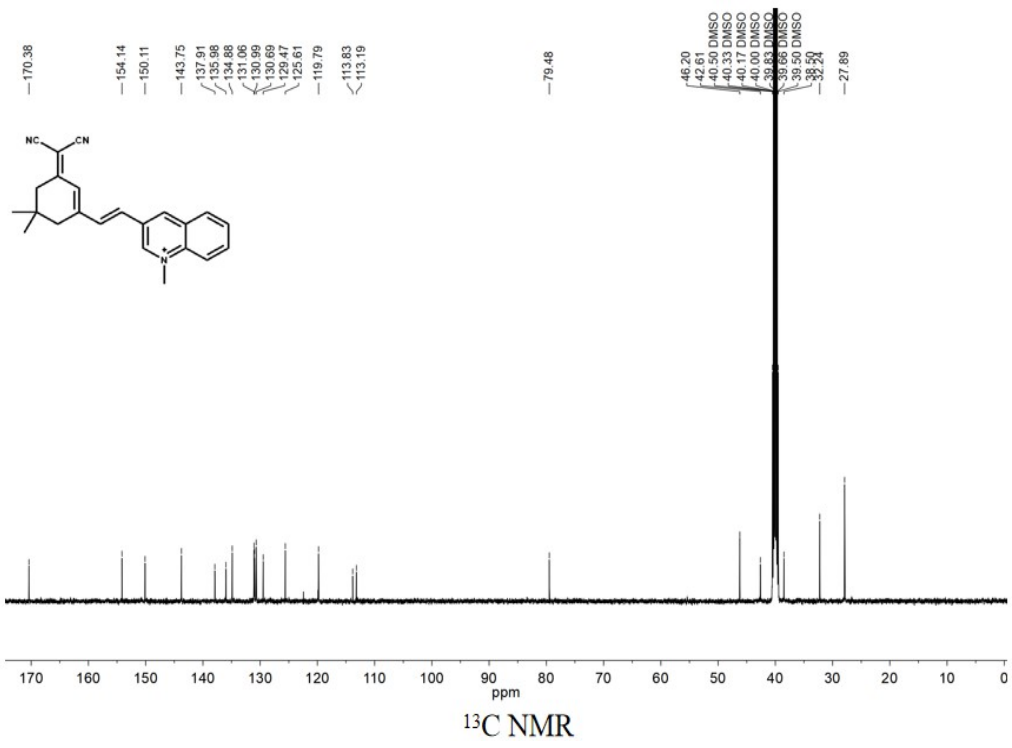

Fig. S16. ^{13}C NMR spectrum of **DCQN** in DMSO-d_6 (126 MHz).

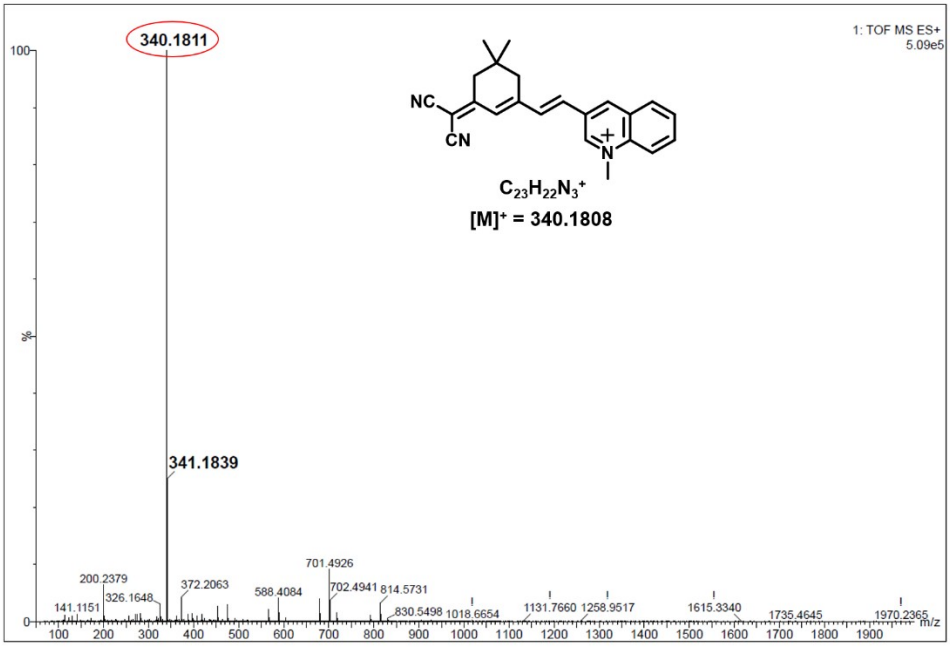

Fig. S17. HR-MS spectrum of **DCQN**.

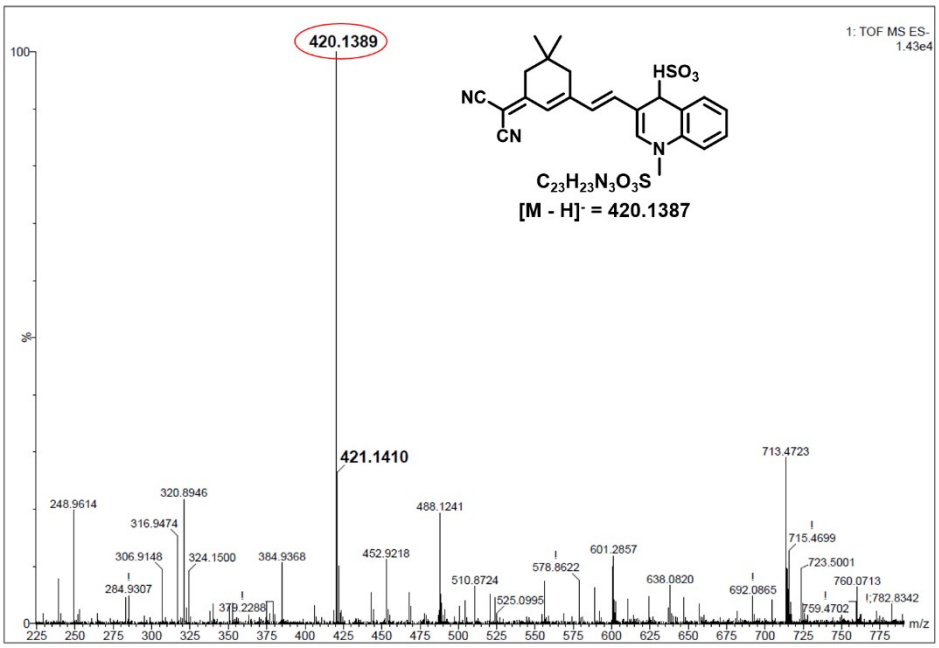

Fig. S18. HR-MS spectrum of **DCQN-HSO_3**.

References

1 J.C. Xu, J. Pan, X.M. Jiang, C.Q. Qin, L.T. Zeng, H. Zhang, J.F. Zhang, *Biosensors and Bioelectronics.,* 2016, **77**, 725-732.

2 L.Z. Yue, H.W. Huang, W.H. Song, *Chemical Engineering Journal.*, 2022, **431**, 133468.

3 H. Li, X. Zhou, J. Fan, S. Long, J. Du, J. Wang, X. Peng, *Sens. Actuators B.*, 2018, **254**, 709–718.

4 X. Yang, Y. Yang, T. Zhou, M. Jin, X. Jing, & W. Li, *Journal of Photochemistry and Photobiology A: Chemistry*., 2019, **372**, 212-217.

5 K. Bi, R. Tan, R. Hao, L. Miao, Y. He, X. Wu, J. Zhang, X. Rui, *Chinese Chemical Letters.,* 2019, 30.3, 545-548.

6 T. Niu, T. Yu, G. Yin, H. Chen, P. Yin, H. Li, *Analyst.,* 2019, **144.5**, 1546-1554.

7 J. Li, Y. Gao, H. Guo, X. Li, H. Tang, J. Li, Y. Guo, *Dyes and Pigments.,* 2019, **163**, 285-290.

8 Y. Zhang, L. Guan, H. Yu, Y. Yan, L. Du, Y. Liu, M. Sun, D. Huang, S. Wang, *Analytical chemistry*.,2016, **88.8**, 4426-4431.

9 Y. Yao, Q. Sun, Z. Chen, R. Huang, W. Zhang, J. Qian, *Talanta.,*2018, **189**, 429-436.

10 G. Zhang, R. Ji, X. Kong, F. Ning, A. Liu, J. Cui, Y. Ge, *RSC advances.,* 2019, **9.2**, 1147-1150.

11 Y.P. Liu, T.B. Ren, D. Cheng, J.N. Hou, D.D. Su, L. Yuan, *Chemistry Open.*, 2019, **8.10**, 12511257.

12 L.M. Zhu, J.C. Xu, Z. Sun, B.Q. Fu, C.Q. Qin, L.T. Zeng, X.C. Hu, *Chem. Commun*., 2015, **51.6**, 1154–1156.